American Mineralogist, Volume 83, pages 970–984, 1998

Solid-solid reactions mediated by a gas phase: An experimental study of reaction progress and the role of surfaces in the system olivine+iron metal

Ralf Dohmen,* Sumit Chakraborty,† Herbert Palme, and Werner Rammensee

Institut für Mineralogie und Geochemie, Universität zu Köln, Zülpicher Strasse 49b, 50939 Köln, Germany

Abstract

The intergranular fluid involved in solid-solid reactions is tacitly assumed to be a melt or a (C-O-H-S-Cl-F)-bearing phase. We have studied the system olivine+metal using diffusion couple experiments, in situ reaction progress monitoring using Knudsen-cell mass spectrometry, and thermodynamic-kinetic analysis to show that a dry vapor phase coexisting with solids (silicates, oxides, metals) has all the characteristics of a classical petrologic ''intergranular fluid,'' and it is a viable transport agent for major rock-forming elements such as Mg, Fe, or Si in many petrologic situations. Some of the major conclusions of the work are: (1) ignoring the vapor phase leads to incorrect estimation of degrees of freedom and consequently, incorrect interpretations of mineral assemblages and zonation; (2) normally refractory elements such as Mg may in some cases be more volatile than O_2; and (3) reaction modeling using free-energy minimization allows the main parameters controlling reaction progress, pathway, and products (assemblage, abundance of phases, and composition) to be identified. These parameters include: available reactive surface area; volume of the reaction system; diffusion rates in the product solid; temperature; and relative rates of reaction to transport (in/out of the system). Components other than those appearing explicitly in the mass-balance equations (e.g., f_{O_2} in the olivine+metal system) may play an important role. Transport of Mg in the vapor phase away from local reaction sites explains the compositional zoning of olivine around FeNi-metal inclusions and simultaneously provides a mechanism for the growth of at least some of the fayalite-rich rims in Allende and other meteorites of the CV3-class. Similar considerations may play a role in terrestrial problems where metal and silicate coexist, e.g., the primitive terrestrial magma ocean and the ''D'' layer.

Introduction

Solid-state reactions that occur during metamorphism of rocks and meteorites are generally thought to progress by diffusion through crystal volumes, grain boundaries, or surfaces, and petrologic interpretations are typically constrained to fit this conceptual framework. However, as detailed studies of pathways of chemical change through the observation of frozen compositional gradients (mineral zonation in the form of bands, corona, etc., as well as chemical zoning within crystals) are becoming widespread, it appears that diffusion alone cannot explain the observed compositional variations in all cases.

A striking example of a problematic case where it is difficult to explain the compositional zoning may be found in the Allende Meteorite. Inclusions of metallic Fe (with Ni) in olivine have halos of iron enrichment around them that are visible in backscattered electron (BSE) images (e.g., Hua et al. 1988; Weinbruch et al. 1990). Chemical analyses and profiling show that these zones of iron enrichment consist entirely of stoichiometric olivine with increasing Fe content as the metallic inclusion is approached. Explaining these features in terms of a conventional diffusion-exchange model is difficult, because if the olivine is to become Fe rich through diffusive exchange with the metal inclusion and remain stoichiometric, Mg must somehow be lost. The corresponding magnesium enrichment in the metal phase is neither expected from considerations of solubility of Mg in Fe, nor observed as some kind of disequilibrium feature (Weinbruch et al. 1990). This indicates that some process, not commonly considered in interpreting reactions between solids, is required to explain the observations.

Other observations, though less striking, reinforce the need for some as yet unconsidered mechanism of reaction between solid phases. For example, it is commonly observed that minerals are zoned toward the rim in a particular component, even when this component cannot enter the immediately adjacent phase in significant amounts. An example of such behavior is the zoning of Ca in olivine toward rims in contact with metal in meteorites (e.g., Zipfel et al. 1995) or with spinel in mantle xenoliths (e.g., Zipfel and Wörner 1992). Similar zoning of Fe/Mg in garnet in contact with quartz or plagioclase can be

* Dohmen@min.uni-koeln.de
† Sumit@min.uni-koeln.de

0003–004X/98/0910–0970$05.00

observed in crustal metamorphic rocks (e.g., O'Brien 1997; Erambert and Austrheim 1993).

The mechanism of transport in such cases must be either through grain boundary diffusion or by transport through an ''intergranular fluid phase.'' In general, there is no direct evidence to suggest that the mode of transport through the intergranular space is indeed grain boundary diffusion, and the physical nature of the hypothetical ''intergranular fluid phase'' is not clear. Clearly, the solubility of critical elements in this ''intergranular fluid phase'' is an essential factor in controlling reaction progress and it is an important parameter for reaction modeling. This role of the intergranular fluid phase was discussed in the classic work of Orville (1963), while earlier Orville (1962) had discussed explicitly the very general nature of such an ''intergranular fluid phase'' (see also Carmichael 1969; Fisher 1973; Foster 1977; Loomis 1976, 1977, 1979). Unfortunately, the original experiments of Orville (1963) were carried out—coincidentally, from the present perspective—in the presence of an aqueous vapor. This left the impression that vapor-phase transport was significant only in the presence of an aqueous vapor—a belief that has deeply influenced petrologic analysis in the subsequent decades.

To explore mechanisms of reaction between solid phases mediated by a fluid phase, we have done 1 atm experiments under controlled f_{O_2} and Knudsen-cell experiments with the system olivine+metal along with thermodynamic and kinetic analysis of the data. The ''intergranular fluid phase'' of interest in our experiments is the simplest and most general one conceivable—a vapor phase generated by solids. The Knudsen-cell mass spectrometer enables one to monitor the fluid composition continuously and in situ as a function of reaction progress. We have chosen to study the system olivine+metal because there are adequate thermodynamic and kinetic data available to characterize adequately the observations, because of experimental convenience, and because of its wide relevance. In addition to providing an explanation for the enigmatic compositional zoning in olivine from the Allende meteorite, data from the present system may be pertinent to understanding features in other meteorites and processes that may have occurred in the early magma ocean on the Earth before the segregation of the metallic core. To the extent that the system represents a model metal/non-metal pair, studying the behavior of this system is conceptually useful for modeling processes occurring at the present-day core-mantle boundary region within the Earth. At the most general level, results from this study should serve as a reference frame against which pathways of other solid-solid reactions may be interpreted and evaluated. Understanding the mode of element exchange between two solids through such studies is a prerequisite for geospeedometry, where it is necessary to define the initial and boundary conditions to the diffusion equation.

In this work, it is shown that the ''intergranular fluid phase'' may be totally unrelated to an aqueous, molten, or carbonaceous/sulfurous/halogen-rich phase (the only kinds of fluids usually considered in petrologic analysis), and this phase is characterized chemically in a reasonably well-constrained experimental system. We demonstrate how reaction path and progress may vary drastically depending on the properties of this fluid phase (abundance and chemistry of the fluid as well as the accessible solid surface area). After reporting the experimental results, we present a simplified thermodynamic-kinetic model to simulate the general behavior and explain some essential observations.

1 ATM EXPERIMENTS

The earliest working hypothesis regarding Allende olivine was that because Mg cannot enter the metal phase, the observed FeO zoning around NiFe-inclusions in olivine is not the result of reaction between included metal and the host. Such a possibility may arise because some of the same olivine shows the development of fayalitic rims far removed from NiFe-inclusions (e.g., Hua et al. 1988; Weinbruch et al. 1990). To test if Fe-Mg exchange is possible even if olivine coexists with Fe metal for long enough times at high temperatures, we carried out a diffusion couple experiment at 1300 °C, $f_{O_2} = 10^{-12}$ bar (which is below the Fe-FeO reaction curve, so that Fe does not oxidize) for 115 h in a 1 atm gas-mixing furnace where the f_{O_2} is controlled by a flowing gas mix of $CO+CO_2$. Chakraborty (1997) describes details of the setup and the precision in controlling various experimental parameters. The experiment duration was chosen such that at the same conditions, two olivines of different compositions pressed against each other showed diffusion profiles 60 μm long after the anneal (Chakraborty 1997). The diffusion couple in the present study consisted of a single crystal of synthetic forsterite (Fo_{100}, details in Chakraborty et al. 1994 and Chakraborty 1997) with a surface perpendicular to [001] polished and pressed against a slab of pure iron metal (99.999%, Heraeus). The two solid pieces were pressed against each other by a spring-loaded alumina setup and were exposed in all directions to the furnace atmosphere. A thermocouple and a solid state zirconia sensor positioned adjacent to the interface monitored T and f_{O_2} continuously. For the purpose of this study, it is important to note that in this ''containerless'' setup using single-crystal silicate blocks, there is no possibility of any contamination or other influence from container material. After the anneal, the entire sample was embedded in epoxy, sectioned longitudinally, and studied under the microscope and using the imaging and analytical capabilities of an electron microprobe (Cameca SX-50 at Bayerisches Geoinstitut, Bayreuth). The major benefit of this method is that the distribution of phases and composition is simple and can be mapped easily, and there is no possibility of missing ''hidden'' components located along grain boundaries or interfaces.

Observations

To our surprise, BSE imaging as well as mapping of fluorescent X-rays showed a pronounced penetration of

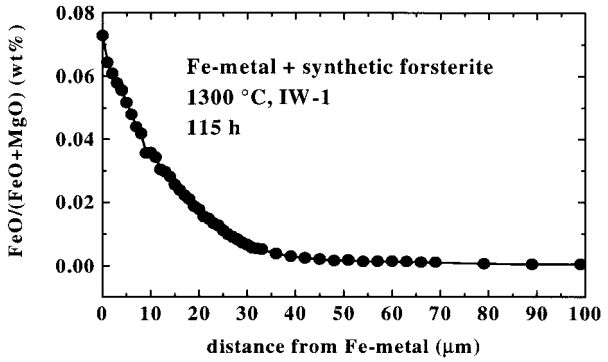

FIGURE 1. FeO concentration profile in forsterite from diffusion couple experiment. The composition at each point along the profile is that of stoichiometric olivine.

Fe in olivine along a well-defined front parallel to the original interface. Chemical analyses revealed that the silicate was stoichiometric olivine at all places. Typical diffusion profiles of Fe could be measured in the olivine (Fig. 1), which are similar to the profiles measured in Allende (Hua et al. 1988). The penetration depth of this profile is consistent with known Fe-Mg interdiffusion rates in olivine at these conditions, as determined recently (Chakraborty 1997). The iron metal was found to contain no significant amount of Mg; there was clearly a missing mass of Mg relative to the original starting materials.

Interpretations

These observations led us to consider three possible alternatives: (1) faster diffusion rates in metal had distributed Mg in the metal over a large region at low concentrations below the detection limit of the electron microprobe; (2) there is a thin, optically undetected layer of magnesiowüstite, which formed at the interface; and, (3) Mg had been lost as a vapor phase to the furnace atmosphere and was subsequently flushed out with the flowing $CO+CO_2$ gas mix.

Alternative (1) was eliminated by repeating the experiment described above with a thin foil of Fe instead of a large block, which yielded the same results. Oxide formation, as outlined in alternative (2), is unlikely because it would not be adequate for mass balance and because the conditions were kept reducing enough to prevent the oxidation of Fe. Nevertheless, to test for alternative (2), we carried out an experiment in which we placed a mix of iron metal powder and forsterite powder in an alumina crucible at 1600 °C and a reducing atmosphere (f_{O_2} = 10^{-11} bar). At these conditions, Fe metal is molten but wüstite is not. After the experiment, we recovered a metal globule, clearly indicating that the Fe was molten (and hence un-oxidized) during the experiment. In this metal globule were pieces of brown, Fe-rich olivine instead of the initial white forsterite. Microprobe analyses confirmed that the initial forsterite had been converted to Fe-rich olivine during the experiment. Thus, we were left with alternative (3) as the only viable explanation of our observations. However, a different experimental setup was needed to document the escape of Mg in the vapor phase. Knudsen-cell mass spectrometry, with its ability to analyze product gases, is ideally suited for this.

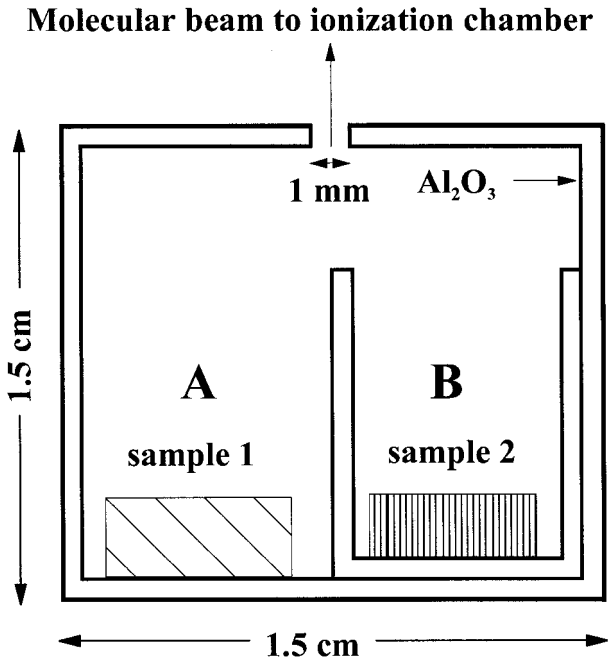

FIGURE 2. Schematic drawing of the sample configuration in the Knudsen cell.

KNUDSEN-CELL EXPERIMENTS

Setup

The principles of Knudsen-cell mass spectrometry (KMS) along with details of the equipment have been described elsewhere (Rammensee and Fraser 1981; Fraser and Rammensee 1982; Rammensee 1988). We provide here only a brief outline focussing on subsequent modifications and some special aspects of the setup for the present study. The essence of a Knudsen cell (Fig. 2) is a sample container, which is well-shielded and surrounded by heaters and diffusers, such that the entire surface of the cell can attain a uniform temperature. In the present setup, temperatures were measured using a sheathed Pt-6%Rh/Pt-30%Rh-thermocouple and a proportional-integral-differential (PID) temperature controller, and the entire cell plus heater system was held at a vacuum of 10^{-8}–10^{-10} bars. When a solid sample contained in the chamber is heated, a vapor phase is generated. This vapor phase can escape through a small hole in the lid of the container, and the resultant effusing molecular beam is then analyzed by a quadrupole mass-spectrometer. In the typical application, effusion rates are low enough that equilibrium between the gas phase and the solid sample is not disturbed, and the measured ion current of a particular gas species is proportional to its partial pressure:

$$P_i(T) = C_i \cdot I_i(T) \cdot T \quad (1)$$

TABLE 1. Details of Knudsen-cell mass spectrometry experiments and experimental products

Experiment	Starting materials and configuration		Thermal history*	Experimental products
	Pos. A	Pos. B		
V892	Fe + Fo_{100} (syn., poly cryst.)	—	(a) heat to 1400 °C (5 °C/min) (b) heat to 1400 °C (5 °C/min) (c) anneal at 1400 °C for 24 h	Fa_6Fo_{94} Homogeneous grains
V893	Fo_{100} (syn., polycryst.)	—	(a) heat to 1500 °C (5 °C/min)	Fo_{100}, single phase
V914	Fe (syn., polycryst.)	Fo_{100} (syn., polycryst.)	(a) heat to 1400 °C (5 °C/min) (b) heat to 1400 °C (5 °C/min) (c) anneal at 1400 °C for 19 h	Fa_2Fo_{98}-Fa_4Fo_{96} Individual grains unzoned
V929	Fe + wüstite (syn., polycryst.)	Fo_{100} (syn., polycryst.)	(a) heat to 1400 °C (5 °C/min) (b) anneal at 1400 °C for 22 h (c) heat to 1400 °C (5 °C/min)	$Fa_{26}Fo_{74}$ Individual grains unzoned†
V932	Fe + wüstite (syn., polycryst.)	San Carlos olivine (single crystal)	(a) heat to 1400 °C (5 °C/min) (b) anneal at 1400 °C for 20 h	Fayalitic films†
V933	Fe (syn., polycryst.)	Fo_{90} + Fo_{100} (syn.) (single crystals)	(a) heat to 1400 °C (5 °C/min) (b) anneal at 1400 °C for 23 h	Fayalitic films
V937	Fe + magnetite (syn., polycryst.)	Fo_{100} (syn., polycryst.)	(a) heat to 1400 °C (5 °C/min) (b) anneal at 1400 °C for 20 h	Molten sample: $Fa_{74}Fo_{26}$†

* Always cooled at 20 °C/min.
† Spinel formation on alumina crucible cell.

where $P_i(T)$ is the partial pressure of species i at temperature T, C_i is a species- and equipment-dependent constant, and I_i is the measured ion current of species i. In general, partial pressures between 10^{-10} to 10^{-3} bars constitute the measurable range for the present equipment. Even during approach to equilibrium, the identity of the gas species and the instantaneous vapor pressure in the cell can still be determined, as in this study, although the measured ion currents do not reflect final, equilibrium partial pressures. This ability to characterize rapidly and continuously the instantaneous states is the essential attribute that allows the Knudsen cell to be used to monitor reaction progress. In this study, the Knudsen cell was used in this mode.

A notable modification for this study was the use of a double-crucible setup for the Knudsen cell in most of our experiments, as illustrated in Figure 2. In this setup, the usual crucible used as a Knudsen cell contains another smaller crucible so that two different solid/molten samples may be introduced, which are not in physical contact with each other. However, both of these samples contact the same gas phase, because the gas is well mixed within the Knudsen cell.

Experiments

The present setup serves two purposes simultaneously: (1) we can place olivine in the inner crucible and iron metal in the outer crucible, so that any reaction can only proceed through the mediation of the gas phase; and (2), we can replace iron metal by suitable mixtures of metal and oxide (Table 1) and thereby study the behavior of the system under different ranges of f_{O_2}. Thus, Fe can play the dual role of a reactant as well as a buffering component in such a setup. Two kinds of olivine samples were used in the smaller crucible with the objective of studying different aspects of the reaction. Powdered forsterite samples were used in experiments where the main objective was to obtain the maximum extent of reaction and possibly attain equilibrium compositions. Oriented single crystals of olivines (forsterite, Fo_{100}, or San Carlos olivine, Fo_{92}), polished on one side, were used to study the exact mechanism of the reaction. Together, these two systems present extremes in grain size and thereby allowed us to study the role of surfaces in controlling reaction progress.

The thermal history in a typical experiment consisted of heating to 1400 °C at 5 or 10 °C/min, annealing at 1400 °C for a duration of 19–24 h, and subsequent cooling to room temperatures at 20 °C/min. In some cases, a double-annealing procedure was followed whereby the sample was cooled after preliminary heating (to drive off any potentially interfering adsorbed impurities, see below) and then reheated and annealed for longer duration, without taking the sample out of the vacuum chamber of the Knudsen cell in between. Table 1 gives the sample configuration used and the detailed thermal history in various experiments.

All samples were characterized after the experiments using X-ray diffraction (XRD) (mainly to determine the oxidation states of the Fe present) and electron microprobe analysis (EMPA). EMPA was carried out using standard procedures on a Cameca-Camebax at the Institut für Mineralogie und Geochemie, Universität zu Köln, operating at 15 kV, 10–20 nA.

Unfortunately, in the presence of wüstite or magnetite the alumina crucible no longer behaved inertly for the long, high-temperature experiments and reacted to some extent to form Fe-rich spinel. Interpretations and conclusions of this study are not affected by this additional spinel-formation reaction.

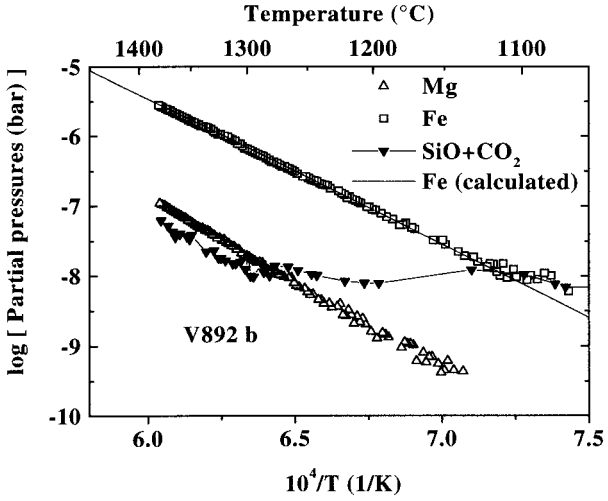

FIGURE 3. Typical gas phase compositions measured during heating in Knudsen-cell experiments with olivine. Also shown are calculated partial pressures of Fe as a function of temperature (solid line), which is used as an internal standard. The slope of this line is the enthalpy change of the reaction Fe (s) = Fe (g).

Treatment of data and calibration

The chemical identity of the species in the gas phase has to be inferred from mass spectrometry. A new PC-controlled measurement system allowed very rapid measurement of ion currents whereby the peaks for several masses could be scanned within a short interval (2 s per peak). This enabled us to identify chemical species by comparing the observed ratios of ion currents with the known natural abundance ratios of different isotopes. In general, the many masses that could be scanned rapidly allowed us to detect and identify most of the major species present in the gas phase. Problems in the direct comparison of ion-current data from various experiments arise from (1) changing sensitivity of the mass spectrometer with time and (2) different geometric factors of different Knudsen cells, which can affect the values of the constant C_i in Equation 1. However, the present experimental setup allowed us to use Fe as an internal standard and overcome these problems.

By differentiating Equation 1 and using ΔG^0 of the vaporization reaction Fe(s) = Fe(g) [with $\ln(K) = \ln(P_{Fe}) = -\Delta G^0/(R\cdot T) = -\Delta H^0/(R\cdot T) + \Delta S^0/R$], it follows that

$$\frac{d\ln(I_i\cdot T)}{d(1/T)} = -\frac{\Delta H^0_{vap}}{R}, \quad (2)$$

i.e., the slope of a plot of ion current times temperature, $I_i\cdot T$, vs. inverse temperature, $1/T$, (ICIT), is proportional to the enthalpy of vaporization of Fe. Comparison of enthalpies calculated from observed slopes from experiments V892, V914, V929, and V937 show that they agree well with literature data (JANAF 1971), as illustrated in Figure 3 for V892. Figure 3 also shows a typical set of observed ion currents for various species in an experiment. X-ray diffraction of the solids showed that when initial Fe was used, most of it remained metallic Fe after the anneal, i.e., conditions within the cell were not oxidizing enough to convert Fe entirely to oxide.

The sensitivity change of the mass spectrometer in a given experiment was not strongly mass dependent, at least within the range of masses from 16 (e.g., O) to 56 (e.g., Fe). This was demonstrated by a calibration with noble gas elements, as described by Rammensee (1988). As the measured enthalpies (slope of ICIT curve) for Fe agree with literature data in each case, it is reasonable to superpose the Fe data at each temperature from different experiments and then compare the vapor pressures of other species on such ''Fe-normalized'' plots.

RESULTS

Experiments with polycrystalline olivine

Olivine composition. The most significant observation from the experiments with polycrystals was that the starting forsterite became enriched in Fe (as fayalite component) at the end of the anneal if Fe was present in the system initially, irrespective of whether this Fe was physically mixed with (e.g., V892) or separated from (e.g., V914, V929, etc.) the olivine (Table 1). The individual olivine grains were unzoned in all cases. However, the compositions of grains from a given experiment were not the same. When a large mass of olivine was taken initially in crucible B, original unreacted compositions were always found in grains from near the bottom of the crucible. Also, in experiment number V914 where a loose mass of forsterite was kept physically separate from the Fe, the grains near the surface showed a scatter in their Fe contents (X^{Ol}_{Fa} = 2–4 mol%), although individual grains were homogeneous. The average Fe content of the product olivine increases with increasing ambient f_{O_2} in the cell. These observations, from experiments such as V914, V929, and V937 where iron metal (with or without oxide) was physically separated from the starting forsterite, document unequivocally that the reaction to produce Fe-rich olivine occurs through the mediation of the gas phase. This also requires that Mg be lost preferentially from the starting olivine relative to Si and O, as we already found from the 1 atm experiments—it remains to be seen in what form and how.

Gas phase composition. In all of the experiments in this study, the gas species become detectable with the KMS above a temperature of about 1100 °C. The dominant gas species coexisting with forsterite (with or without Fe in the system) are SiO, O_2 (O), and Mg, as also observed by Nichols et al. (1995). Generally, in the case of SiO, we have the problem that the ion current of $^{12}C^{16}O_2$ overlaps the $^{28}Si^{16}O$ signal. This distorts the relative proportions of SiO to Mg and O. However, it was possible to identify SiO with the isotopes $^{28}Si^{16}O$, $^{29}Si^{16}O$, and $^{30}Si^{16}O$ at 1400 °C during later stages of an annealing, after CO_2 was degassed (Fig. 4). Heating to 1400 °C, cooling to room temperatures, and then re-heating also allowed the SiO signal to be observed more clearly. The

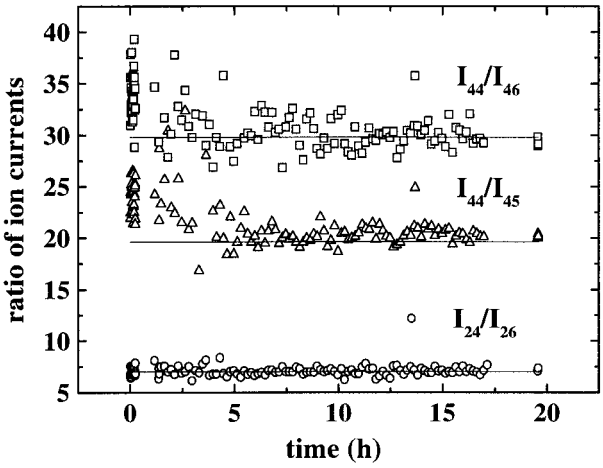

FIGURE 4. Examples of ratio of ion currents observed at selected masses, used to identify the gas species, as a function of duration of experiment. Symbols show measured data and the corresponding solid lines indicate the ratios expected from the natural abundances of isotopes. Results are illustrated for the masses 44, 45, and 46 used to identify SiO(g) and 24, 26 used to identify Mg(g).

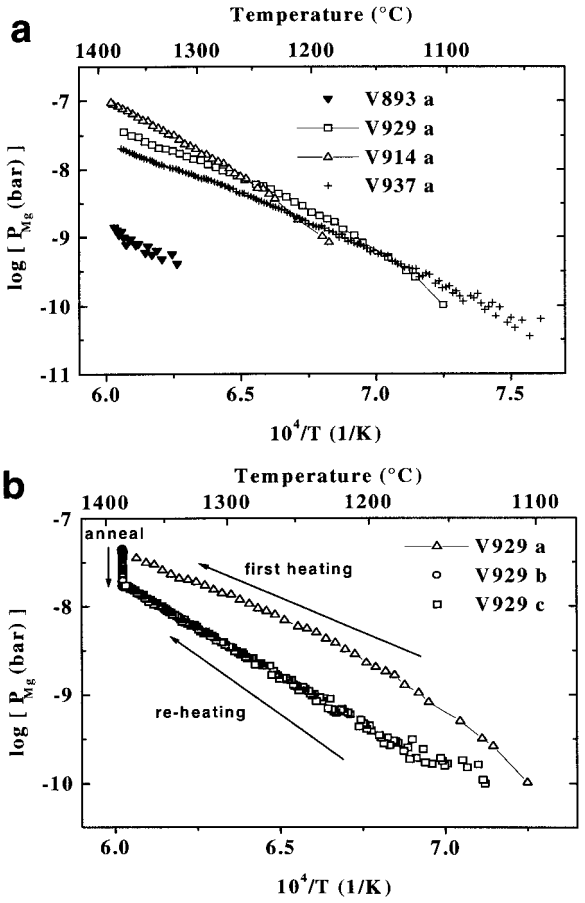

FIGURE 5. Magnesium pressures observed in experiments: (**a**) P_{Mg} observed during first heating of forsterite without (solid triangle) and in the presence of Fe (crosses and open symbols) at different O partial pressures. Note that the initial P_{Mg} are higher for experiments with higher f_{O_2}. (**b**) P_{Mg} for a complete annealing cycle (V929). Note the high P_{Mg} during the first heating; the decay during a constant temperature anneal at 1400 °C; and the relatively low, well-behaved linear P_{Mg} during the second heating, which attains the same "equilibrium" value at 1400 °C as at the end of the anneal.

O_2 pressure at the iron-wüstite buffer is $\sim 2.0 \cdot 10^{-10}$ bar at 1400 °C. Because Fe was not oxidized in experiments V892 and V914, the O_2 pressure must have been even lower. In addition, because the sensitivity limit of the KMS is about 10^{-10} bar, the O_2 pressure could not be detected in experiments V892, V914, and V929.

The behavior of Mg is of course the most interesting one from the perspective of the present study. Unlike SiO and O_2, the Mg signal can be observed clearly because the partial pressure of Mg is well within the detection limits of the KMS at temperatures between 1100-1400 °C, and Mg is present in the gas phase dominantly as an elemental species, unaffected by any serious overlaps. Thus Mg can be identified unequivocally using the ratios of ion currents at masses 24, 25, and 26 (Fig. 4). The most important observation is that the partial pressure of Mg (i.e., concentration in the gas phase) increases dramatically when some Fe is present in the system, irrespective of whether this Fe is in contact with the olivine or not (Fig. 5a). Heating forsterite alone, without any Fe in the Knudsen cell, gives much lower vapor pressure of Mg. The relative strengths of the SiO and Mg signals and the fact that the residual solid at the end of the annealing was single-phase forsterite, as in the starting material, indicates that forsterite evaporates stoichiometrically in this case, as also observed by Hashimoto (1990), Mysen and Kuhiro (1988), and Nagahara et al. (1994). This behavior confirms that during reaction of olivine with Fe, Mg is lost from the olivine to the gas phase.

A further observation is that a difference exists in the behavior of the ICIT curve of Mg between the first and subsequent heating to 1400 °C. During the first heating, the ICIT plot of Mg (Fig. 5a) is curved in experiments where Fe is present, in contrast to the linear behavior for repeated heating sequences (Fig. 5b). Comparing experiments carried out at different values of f_{O_2} (Fig. 5a), we find that a sequence of decreasing P_{Mg} at lower temperatures [P_{Mg}(V914) < P_{Mg}(V929) < P_{Mg}(V937)] corresponds to a sequence of increasing fayalite contents of product olivine [V914 (Fa = 4 mol%) < V929 (Fa = 26 mol%) < V937 (Fa = 70 mol%)] and ambient f_{O_2} in the cell (V914 = iron metal, V929 = iron metal+wüstite, and V937 = iron metal+magnetite). On reaching the final annealing temperature of 1400 °C, irrespective of the previous history, after an initial decrease, the Mg partial pressure picks up and attains a constant value (Fig. 6).

We can conclude from these observations that iron metal reacts with olivine mediated through a gas phase and Mg is lost as vapor, resulting in the production of

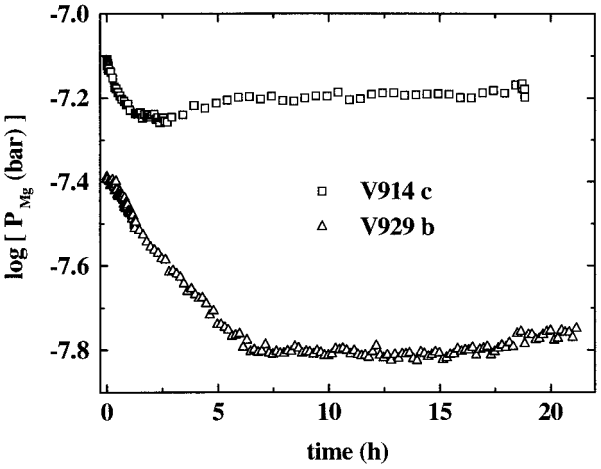

FIGURE 6. The behavior of P_{Mg} during the constant temperature anneal at 1400 °C for two experiments at different values of f_{O_2}. Note the difference in the final ''equilibrium'' value attained in the two cases (V914 and V929).

Fe-rich olivine; the extent of this Mg loss is dependent on ambient f_{O_2}.

It remains to be shown exactly how the Fe is incorporated in the olivine. There are two alternatives: (1) a direct exchange between Fe in the gas phase and Mg in the olivine or (2) stoichiometric evaporation of Mg-rich olivine (with Mg, Si and O) followed by precipitation of a more iron-rich olivine and loss of Mg in the vapor phase. To answer this question, we consider experiments carried out using single crystals of olivine, where the geometry of the reaction system is much better defined.

Single-crystal experiments

These experiments were identical to the experiments with polycrystals, except that the sample consisted of an single cube (2 mm on a side) of an olivine single crystal in which the surface perpendicular to [001] (the fastest diffusion direction in olivine) was ground flat and polished, as for diffusion experiments (see Chakraborty et al. 1994 and Chakraborty 1997 for details). The crystals used were either pieces of synthetic forsterite (white in color, Fo_{100}) or San Carlos olivine (pale green, Fo_{90-92}). The crystals were placed with the polished surface on top in crucible B of the Knudsen cell (see Fig. 2). In one case (V932), two single crystals of both compositions were placed next to, but not touching, each other.

The most remarkable observation in these experiments was that spectacular thick films (up to 300 μm thick) of single-crystal, Fe-rich olivine formed on the original crystals (Fig. 7). These films formed on all surfaces of the single crystals (including the bottom, which was in contact with the alumina crucible) and even along internal surfaces of the single crystal exposed by cracking (e.g., see Fig. 7b); this represents unequivocal evidence of formation from the gas phase. The films were dark in color, with a convex surface and commonly with a prismatic

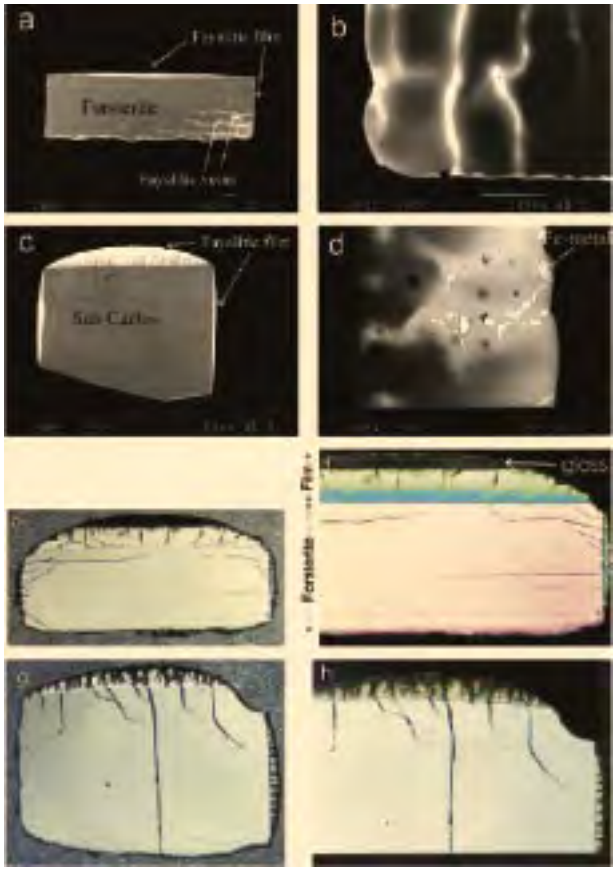

FIGURE 7. BSE images and thin section photomicrographs of single-crystal samples from Knudsen-cell experiments. BSE of forsterite (**a**) and San Carlos olivine (both experiment V933) (**c**) with thick film of overgrown Fe-rich olivine; (**b**) and (**d**): enlargement of fayalite-rich regions in (**a**) and (**c**), respectively. The darker regions represent the original crystals, all bright regions (on all surfaces as well as in interiors) are newly formed Fe-rich olivines. Analyses at all points yield compositions corresponding to olivine stoichiometry, excepting the extremely bright patches [e.g., in (**d**)], which are iron metal. (**e**) and (**f**) are photographs of thin sections of the same crystal as in (**a**) and (**b**), (**f**) with crossed polarizers and different magnification; (**g**) and (**h**) are the corresponding images for the crystal in (**c**). The thin sections show unequivocally that the overgrown olivine is a single crystal in optical continuity with the substrate. The extreme iron enrichment, leading to the formation of molten olivine (dark glass) near the top of the overgrown film is seen clearly in the photographs with crossed polarizers. The pillared structure of the film is of type Z3 (Smith 1996), typical of growth from a vapor phase at high temperatures. The wavy nature of the substrate/overgrowth contact is evidence of evaporation and subsequent growth of new olivine (the original surface would appear straight at this resolution).

internal structure (Z3 structure in the terminology of thin-film science, see Smith 1996), which is indicative of growth from a vapor phase at high temperatures (Smith 1996). Originally straight edges of the single crystal are seen to become wavy (e.g., Fig. 7f). Observation of thin

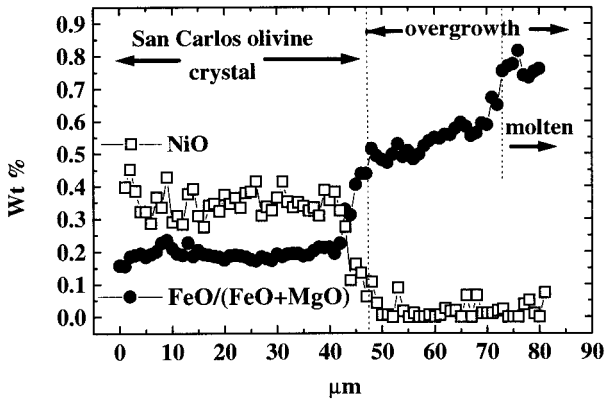

FIGURE 8. Compositional profile across single crystal (San Carlos)/overgrowth interface (Experiment V932). Note the two compositional jumps—one at the interface and the other due to the compositional gap between solidus and liquidus in the olivine system, both modified by subsequent diffusion. Faster diffusion in the melt relative to the crystalline olivine is clearly seen in the much gentler slope of the profile in the molten part. The Ni profile clearly shows that the overgrowth consists of newly grown olivine.

sections from experiment V933 show that the films are made up of olivine that is optically continuous with the substrate and grades into a glassy region near the top of the layer (Figs. 7e–7h). This glass is seen to penetrate and flow through cracks in the film and the substrate. It shows that small volumes of fayalitic glass can be quenched even with cooling rates as slow as 20 °C/min, as in our experiments. There are some Fe-metal particles in the liquid (e.g., Fig. 7b), which may be the products of internal reduction during cooling (e.g., Schmalzried 1995) or simply quench phenomena. All these features show a remarkable similarity to fayalite-rich rims and veins found in olivine from the Allende meteorite (Peck and Wood 1987; Hua et al. 1988; Weinbruch et al. 1990; Krot et al. 1995), although there are differences in detail, e.g., the occurrence of the glassy regions in the experimental samples.

Chemical analysis using the electron microprobe shows that the material has the stoichiometry of olivine at all places, including the glassy region. Pronounced diffusion profiles occur between the substrate and the coating, with compositions becoming more Fe rich away from the substrate (Fig. 8). In the olivine of Experiment V932, the boundary of the unreacted part of the starting crystal and the newly formed film is well marked by the jump in the Ni content (original crystal ≈3000 ppm; film <100 ppm).

DISCUSSION

Reaction mechanism and thermodynamic analysis

The fact that the newly formed olivine has a distinctly different, undetectable Ni content (but variable Fe content) allows us to identify the mechanism of reaction and choose between the two alternatives mentioned above. A simple exchange of Fe for Mg would not alter the shape of the crystals and the Ni content in the Fe-rich and Fe-poor olivine would be the same. Thus, we conclude that the formation of the Fe-rich olivine involves the following reaction pathway: initial Mg-rich olivine evaporates and dissociates into Mg, SiO, and O_2

$$MgSi_{0.5}O_2\ (s) \rightarrow Mg\ (g) + 0.5\cdot SiO\ (g) + 0.75\cdot O_2\ (g) \quad (3)$$

followed by reaction with iron vapor available in the gas phase and condensation of a more Fe-rich olivine (in equilibrium with the P_{Fe} of the vapor phase)

$$x\cdot Mg\,(g) + (1-x)\cdot Fe\,(g) + 0.5\cdot SiO\,(g) + 0.75\cdot O_2\,(g) \rightarrow (Mg_xFe_{1-x})Si_{0.5}O_2\,(s). \quad (4)$$

Summing the two, the net reaction may be written as

$$MgSi_{0.5}O_2\ (s) + (1-x)\cdot Fe\ (g) \rightarrow (Mg_xFe_{1-x})Si_{0.5}O_2\ (s) + (1-x)\cdot Mg\ (g) \quad (5)$$

or in terms of end-members, the governing reaction is

$$MgSi_{0.5}O_2\ (s) + Fe\ (g) \rightarrow FeSi_{0.5}O_2\ (s) + Mg\ (g). \quad (6)$$

The equilibrium constant, *K*, of reaction 6 is given by

$$K = \frac{X_{Fa}\cdot P_{Mg}}{X_{Fo}\cdot P_{Fe}} \quad (7)$$

where we have replaced activities by partial pressures for gaseous species and mole fractions for components in the solid phase assuming ideal behavior for this simple analysis. From this, we obtain

$$\frac{X_{Fa}}{X_{Fo}} = K\cdot\frac{P_{Fe}}{P_{Mg}} \quad (8)$$

or that the composition of olivine is proportional to the ratio of P_{Fe}/P_{Mg} in the gas phase. Because P_{Fe} is fixed in most cases in our experiments by the coexistence of an ''infinite reservoir'' of Fe, assuming that the rate of the reaction Fe (s) → Fe (g) is rapid, it follows that the Fe content of the olivine is inversely proportional to P_{Mg} in the gas phase; the lower the P_{Mg}, the higher the Fe content of the olivine at equilibrium. Thus, oxidizing f_{O_2} decreases P_{Mg} and P_{SiO} in Equation 3 according to the law of mass action; this decrease in P_{Mg}, in turn, increases P_{Fe}/P_{Mg} of the system to produce more Fe-rich olivine according to Equation 6. This explains the indirect role of f_{O_2} in controlling the Fe content of product olivine.

This simple analysis suggests that the olivine composition in any closed or open system could be dictated entirely by the ratio P_{Fe}/P_{Mg} of the coexisting gas phase. Thus, any process that affects this ratio (e.g., oxidation or a flux of Fe or Mg into or out of the system) affects the olivine composition.

Polycrystal experiments

At 1400 °C, the olivine grains have several hours to equilibrate with the surface conditions by diffusion and therefore the constant vapor pressure of Mg during the

remainder of the anneal (periods of up to 20 h) reflects the attainment of ''equilibrium'' over the bulk of the olivine crystals (''equilibrium'' here refers to a steady-state pseudo-equilibrium because a true equilibrium state cannot be defined for a partially open system). This interpretation is consistent with known diffusion rates for Fe-Mg in olivine (Chakraborty 1997) and observed grain sizes of 5–10 μm. The observation of homogeneous olivine crystals, all of similar compositions, at the end of the long anneals at the relatively high temperature of 1400 °C also supports this interpretation.

Note that the absolute values of P_{Mg} at a given temperature are higher during the first heating (Fig. 5b). This is consistent with our interpretation that, during the first heating, the gas phase is that obtained from evaporation of more Mg-rich olivine surfaces that are evolving toward the ''equilibrium''Fe-rich composition. During the first heating, the observed vapor pressure of Mg is that due to evaporation of Mg from the surface of the forsterite grains in contact with an Fe-vapor phase. The vapor pressure of Mg in this case is higher than that due to simple evaporation of forsterite. The relatively small volume of the cell is, however, quickly saturated with Mg in the vapor phase and it is the effusion of vapor, with some Mg in it, that allows further incremental reaction progress, i.e., conversion of forsterite to more Fe-rich olivine. The decreasing forsterite content in the olivine surface lowers the P_{Mg} according to reaction 3. Additional corroboration of the inference that the curve in ICIT is related to disequilibrium resulting from sluggishness of the olivine-forming reaction comes from the observations that (1) for heating forsterite only (without Fe in the system), no such kinks were observed and (2) when the iron powder is intimately mixed with the forsterite (e.g., V892) rather than physically separated, the magnitude of this kink is much smaller and the ''equilibrium'' P_{Mg} at 1400 °C is attained much more quickly.

The slope of ICIT during the second heating cycle represents P_{Mg} in ''equilibrium'' with the final olivine composition. This can be verified by using the final, measured olivine compositions X_{Fa} and the P_{Fe} coexisting with metallic Fe at a given temperature to calculate, using Equation 7, P_{Mg} as a function of temperature. Excellent agreement between calculated variations of P_{Mg} with temperature and measured data (Fig. 9) substantiate our interpretations on a quantitative basis.

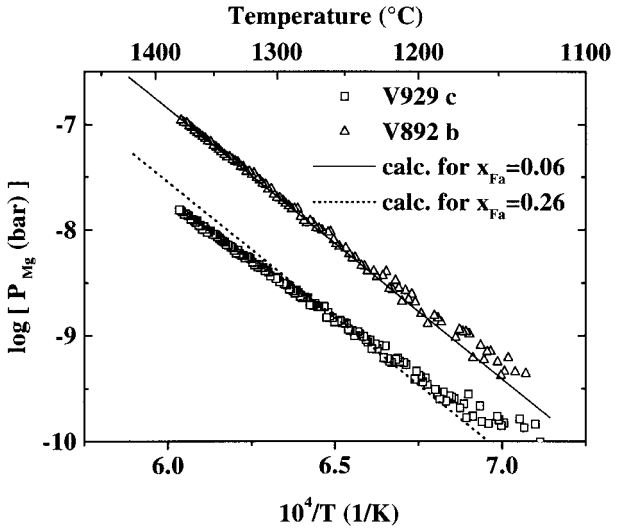

FIGURE 9. Partial pressure of Mg during experiments at two different f_{O_2}. Measured data are shown as symbols and solid lines are the results of calculation using thermodynamic data for the corresponding cases. In view of the excellent agreement of the two slopes, the calculated partial pressures were used to convert the observed ion currents for Mg to absolute values of partial pressure (i.e., to determine C_{Mg} of Eq. 1).

Polycrystal vs. single crystal

The most Fe-rich olivine near the surface is almost end-member fayalite (Fa_{95}) in the single-crystal experiments. The preceding analysis now helps to explain why the iron-enrichment trend in the single-crystal experiments is much more pronounced compared with the polycrystal experiments. We can visualize the process as a continuous sequence of evaporation-condensation steps, where the amount of olivine evaporating or condensing in a given step decreases progressively with time as the system approaches ''equilibrium.'' In between each of these infinitesimal steps, the vapor phase leaves the Knudsen cell by effusion. According to the mechanism deduced above, after initial evaporation from forsterite and reaction with iron vapor in the gas phase, a somewhat Fe-rich olivine is condensed onto the surface of the single crystal. Subsequently, effusion out of the cell depletes the gas phase of Mg, making the gas phase unsaturated in Mg. This behavior is the key difference with the polycrystalline case, where the large available surface area of olivine did not allow the depletion of Mg to proceed to such an extent and consequently drove the key parameter, P_{Fe}/P_{Mg}, and reaction progress along a different path. The depletion of the gas phase causes an evaporation of olivine from layer 1 and subsequent formation of olivine even richer in Fe (layer 2). This sequence continues through the entire duration of the experiment, so that subsequent layers are always richer in Fe resulting in the extreme iron-enrichment trend. This process is documented by lower measured P_{Mg} during heating for the single-crystal experiments compared to the polycrystal experiments (Fig. 10).

This process of producing more Fe-rich olivine continues until at some point olivine with Fe content greater than Fa_{40} are produced, which is molten at 1400 °C. At this stage, a liquid forms rather than a crystalline precipitate; however, the thermodynamics of the system follows the same course. This explains the occurrence of the glassy region. Thus, a disequilibrium path is followed for the single-crystal experiments where the escaping gas phase is unsaturated with Mg, in contrast to the polycrystal experiments and therefore the reaction products

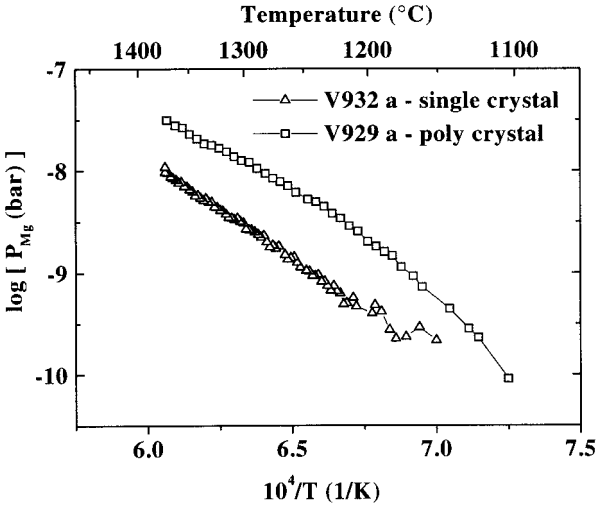

FIGURE 10. Comparison of partial pressure of Mg during heating of single-crystal (triangle) and polycrystal (square) samples. The low P_{Mg} seen for the single-crystal sample shows that the cell was not saturated with P_{Mg} during these experiments.

are more strongly dependent on initial conditions (abundance and composition of olivine). This is seen clearly in experiment V932 where two single crystals of olivine (Fo_{100} and Fo_{92}) were used simultaneously. The trend of iron enrichment is the same in both, as discussed above. However, the exact compositions of the new olivine that forms (i.e., the reaction pathway) are different for the two different starting compositions. If a pseudo ''equilibrium'' was attained, as in the polycrystal experiments, then one would expect the compositions of products on these two olivine crystals to be the same.

Simultaneously with the reactions occurring on the surface, diffusion from the interior of the olivine crystals modifies the composition of layers 1, 2, etc. The diffusion profiles (Fig. 8) across the interface clearly document this reaction pathway. The two most conspicuous features of this profile are: (1) the fact that the trend of iron enrichment continues within the newly grown film, i.e., the profile does not flatten out, in contrast to that of Ni; and (2) that there are two jumps in composition, or ''compositional boundaries'' instead of one. The first feature is exactly what we would expect from the simple thermodynamic analysis above. The second feature is explained as follows: The first compositional jump corresponds to the discontinuity between the compositions of the starting olivine and the first, newly formed olivine (determined by the relative volumes of the reactants and the mediating gas phase). The second compositional jump simply documents the compositional gap between the solidus and liquidus of olivine at 1400 °C (i.e., documents the fact that coexisting solid and liquid olivine do not have the same compositions at a given temperature). Of course, both of these compositional jumps have been modified and moderated by subsequent volume diffusion during the anneal at 1400 °C.

The difference in the Fe content of olivine observed at the end of essentially similar experiments using polycrystals or single crystals is directly related to the surface area available for reaction. The larger surface-to-volume ratio in the polycrystalline samples resulted in the composition of the olivine converging to a homogeneous, ''equilibrium,'' steady-state value. In contrast, the restricted surface area of the single crystals caused the interiors of the crystals to become easily shielded by the successive formation of new films of olivine. This resulted in a continuous change of the reactive bulk composition of the system, so that zoned olivine was formed without converging to any constant value. This behavior is quantified below, but the difference demonstrates conclusively how available surface area (caused by the extreme variation in grain sizes in this case) can change the pathway of reaction, the extent of reaction, and thereby, the ultimate products that are observed (viz., more Fe rich and zoned olivine).

REACTION MODELING

Based on the preceding interpretations and thermodynamic analysis, we have applied detailed reaction modeling to simulate some aspects of the behavior of the partially open Knudsen-cell setup and to quantify some of the earlier observations. Such quantitative modeling allows us to identify parameters that are important for reaction progress and to carry out a sensitivity analysis.

Method

Figure 11 illustrates schematically the reaction system with all kinetic processes involved. The system is characterized by six processes occurring at rates R_1 through R_6, with R_3, $R_6 << R_1$, R_2, R_4, R_5 (R_i defined in the caption of Fig. 11). The sluggishness of intracrystalline diffusion and gas flux out of the system relative to the other processes implies that the total evolution of the system may be broken down into two steps: a rapid, closed-system ''reaction'' step where the gas phase reacts with the solid surfaces (processes R_1, R_2, R_4, R_5); and a second, open-system ''transport'' step (dominated by R_6). R_3 is considered to be too slow and is ignored in the preliminary simulations carried out here. To simplify the simulation further, we have assumed total loss of the available gas phase from the cell at each ''transport'' step, and the evolution of the bulk system was modeled as an iterative sequence of such ''reaction'' and ''transport'' steps. At each ''reaction'' step, the bulk composition, the phase assemblage (olivine+magnesiowüstite+metal+vapor), the volume (V) and the temperature (T) were considered to remain constant and the non-stoichiometric formulation of chemical equilibrium calculation (e.g. Smith and Missen 1991; Abbott and Van Ness 1972) was used to obtain the abundance of each phase and its composition for a thermodynamically closed system. The minimization of G with constant T, V, with a given choice of equation of state for the gas phase, is equivalent to the minimization of the Helmholtz free energy, the correct

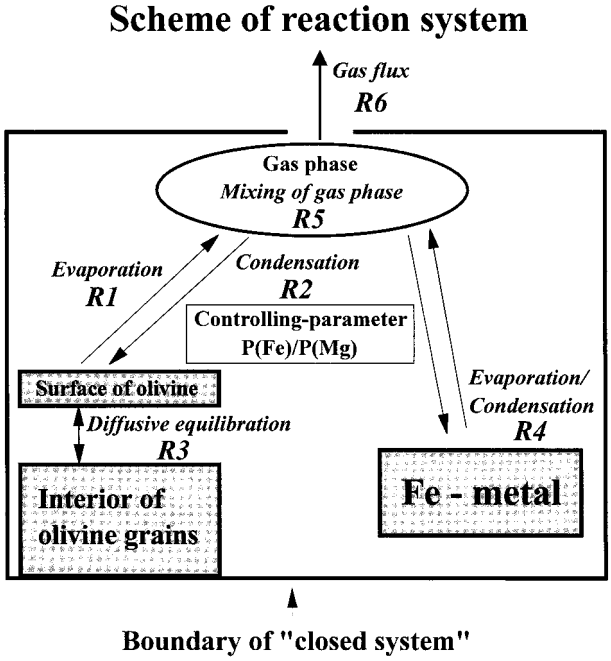

FIGURE 11. Schematic drawing of the reaction system showing the various processes involved. The thick line marks the boundary of the reaction volume, within which the samples react toward ''equilibrium'' under closed system conditions. The relevant processes for understanding the evolution of the system (with the rate for stage *i* denoted by R_i) are: (1) evaporation from the surface of olivine; (2) condensation of new olivine from gas phase; (3) equilibration of interior of olivine grain with surface concentration by intracrystalline solid state diffusion; (4) evaporation of iron metal; (5) mixing and reaction of species in the gas phase; and (6) flux of gas phase out of the reaction volume by Knudsen effusion. Processes 1, 2, 4, and 5 occur during the ''reaction'' step of our model and process 6 is the ''transport step.'' Process 3 is the slowest of all and is neglected in our reaction modeling using zeroth level approximation used in this study. R_1, R_2, R_4, R_5, are considered to proceed instantaneously without any kinetic inhibition in this version of the model.

potential for a system with constant *T* and *V* (Smith and Missen 1991). In the immediately following ''transport'' step, the gas phase was allowed to escape from the system (thereby simulating the partially open Knudsen cell in the experiments and metasomatism in nature), and the bulk composition of the system was updated accordingly. The kinetics of solid-gas reaction was not taken explicitly into account (R_1, R_2), and it was assumed that given enough surface area, the reaction proceeds instantaneously. The effect of variable surface area was simulated by changing the effective reacting volume of olivine and/or Fe in the system.

The system modeled is Mg-Fe-Si-O with Fe-Mg olivine, iron metal, and magnesiowüstite [$Fe_{(1-x)}Mg_xO_{1+z}$] as the solid phases and a gas phase with the nine species: Fe, FeO, Si, SiO, SiO_2, Mg, MgO, O_2, and O. The standard Gibbs free energies of formation were taken from JANAF (1971) and Robie et al. (1979). For fayalite, we have to extrapolate ΔG^0 of the crystalline phase well above the melting point at 1490 K. The gas phase was taken to be ideal and activities of olivine and magnesiowüstite were calculated using data from Wiser and Wood (1991) and Srecec et al. (1987), respectively. These data were chosen because they are specifically valid for the conditions where magnesiowüstite coexists with metallic Fe.

A typical simulation starts with pure forsterite and Fe as the solid phases. After the first ''reaction'' step the compositions and abundances of all phases change (Fe-bearing olivine and magnesiowüstite are formed) depending on the *V* and *T* of calculation and the initial abundance of phases (chosen as free input parameters). The gas phase is allowed to escape in the subsequent ''transport'' step and the calculation is repeated with products from the first reaction step as the reactants, the sequence is repeated until the end of the simulation. (See Appendix 1[1] for details of the method, e.g., equation system for the ''reaction'' step and numerical results)

RESULTS

Figures 12a–12e illustrate some significant results of the reaction modeling. In these figures, the number of ''transport'' steps is related to time in the real experiments and, after a certain number of ''transport'' steps a steady state is obtained. However, the time necessary to get to this state increases with the starting amount of olivine (Fig. 12a) and decreases with increasing volume, *V*, of the reacting system (Fig. 12b) and temperature, *T* (Fig. 12c). The ''equilibrium'' composition of olivine obtained ultimately depends, on the other hand, on temperature and redox conditions and is independent of the starting olivine composition (Fig. 12d). The approach to steady state in terms of several other variables (partial pressures of various species) is shown in Figure 12e. The similarity between the calculated pattern of evolution of P_{Mg} and the observed evolution of partial pressure of Mg during the annealing sequence (Fig. 6) indicates that by measuring the partial pressure of gaseous species, we can indeed monitor in situ the progress of surface reaction within the cell. The results of the simulation agree with the qualitative deductions made earlier. Two of the more significant results obtained from the quantitative simulations are discussed here in detail.

(1) The ultimate composition of the product olivine depends, in addition to the usual intensive variables *P*, *T*, and bulk composition, on the abundance of various phases in the system at any given stage (Fig. 12a). Although this is a simple consequence of the lever rule in a closed system, the result is obtained here in conjunction with partially open-system behavior. In a partially open system such as the one considered here, the abundance

[1] For a copy of Appendix 1, Document AM-98-015, contact the Business Office of the Mineralogical Society of America (see inside front cover of recent issue for information). Deposit items may also be available on the *American Mineralogist* web site (http://www.minsocam.org).

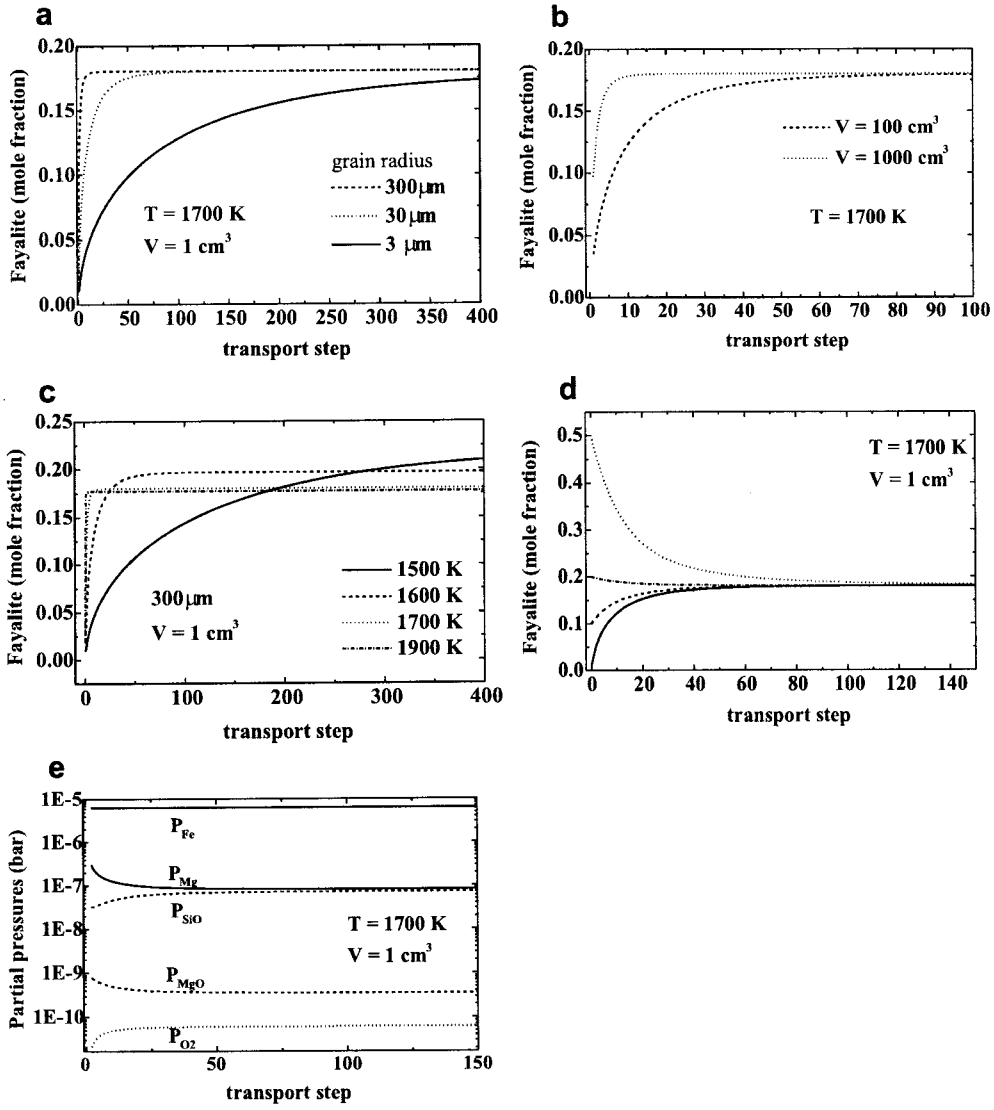

FIGURE 12. Results of simulation studies using reaction modeling as an iterative sequence of ''reaction'' (closed system) and ''transport'' steps. Various parameters are used as monitors of reaction progress in these plots. (**a**) Evolution of fayalite content of olivine with time. The various curves show the role of initial abundance of olivine (surface area of 1.4 mg forsterite) in controlling reaction progress. (**b**) The effect of total volume of reaction system on reaction progress as a function of time. (**c**) The effect of temperature on reaction progress as a function of time. Note that the olivine composition obtained at the end is not a strong function of temperature. (**d**) Evolution of olivine composition with time for different starting compositions. Note that the final olivine composition obtained is independent of starting composition, showing convergence to the ''equilibrium'' value. This behavior is observed for all conditions used for these simulations (see text for further details and exceptions, e.g., for our single crystal experiments). (**e**) Reaction progress monitored through various variables (partial pressures of different gaseous species). Partial pressures for all species converge to the ''equilibrium'' value. Note the similarity in the calculated evolution pattern of P_{Mg} here and the measured ones, illustrated in Figure 6. Also, note the remarkably higher vapor pressures of Mg, Si, and Fe relative to the more ''volatile'' O, contrary to intuition.

of the phases control the composition of the escaping gas phase at each ''transport'' step and therefore, the path of compositional evolution of the system as a whole. Thus, it is possible to obtain very different olivine compositions after a given time merely by changing the initial abundances in the reacting system, with all other parameters remaining constant.

Concerning initial abundances, it is worthwhile to note the special status of the gas phase—its abundance is determined by the size of the system chosen because it fills all available free space. It follows from the ideal gas law that $P_i \cdot V = n_i \cdot R \cdot T$ for any species i in the gas phase, i.e., the partial pressure of i in a system of constant volume, V, is directly proportional to the number of moles of i in

the gas phase at constant temperature. Because equilibrium is determined by equality of partial pressures (in ideal systems), this leads to some interesting consequences. In a given closed volume, V, if the initial abundance of olivine is low (i.e., V_{gas} is high), to attain a given partial pressure requires greater n_{Mg} in the gas phase. If this gas subsequently escapes, Mg is lost from the system. However, if the reaction is carried out in system of smaller volume with the same number of moles of olivine initially (i.e., V_{gas} is low), a smaller amount of Mg would be lost after the same reaction sequence. Therefore, the compositional evolution of such a system is controlled by the size of the system (Fig. 12b). This size dependence remains in an open system (constant P) as well and is a unique feature of reaction systems involving a gas phase. Any partially open behavior or local variations in modal abundances can lead to different reaction paths and products in such systems, and reaction histories may change as the size of the reactive domain changes for some reason.

A second interesting consequence of the dependence of reaction history on abundances relates to the fact that in our simulations, the abundance of olivine is a proxy for available surface area for reaction. Thus, the dependence of product composition on abundance in the simulations (e.g., Fig. 12a) shows that the composition depends on the available surface area. For example, in our single-crystal experiments, the ''effective'' olivine volume that participated in the reactions was very low, although the actual volume of olivine was quite high.

(2) The first point emphasizes the wide range of variability that may arise in such partially open reaction systems. However, the simulations show that if certain restrictions are obeyed, a system with a given set of initial conditions (T and bulk composition) always converges to a fixed ''equilibrium'' olivine composition at the end, irrespective of the starting composition of olivine (e.g., Fig. 12d). These restrictions are: (1) there is no kinetic barrier (i.e., availability of reactive surface area is not an obstacle) and diffusion within solids is not rate limiting (i.e., grain size is small); (2) there is adequate supply of the metal phase; and (3) the gas phase is always saturated during the ''reaction'' stage. This last restriction means that equilibrium is attained between successive ''transport'' stages; in other words, the transport rate (in our case the effusion rate from the Knudsen cell) does not exceed some critical threshold value. Conditions (1) and (3) are related—the governing parameter is the relative rate of equilibration of the solid (stated through condition 1) and transport out of the system, or time scale of open system behavior (stated through condition 3). Experimentally, these conditions are fulfilled in our polycrystalline experiments and we do observe a convergence to a given composition after long anneals at high temperatures. Uncertainties in the thermodynamic data of 1% can yield very distinct ''equilibrium'' olivine compositions in the calculations. For example, a variation of 5 kJ for ΔG^0 of $FeSi_{0.5}O_2$ leads to a variation of $\approx$5 mol% in the ''equilibrium'' fayalite content. Thus, small errors in the thermodynamic data, combined with the various simplifying assumptions made for the reaction modeling, could explain the difference between the experimentally observed ($\sim$6 mol%) and calculated (18 mol%) fayalite contents of the product olivine. Conditions 1 and 3 are not obeyed for the single-crystal experiments and we observe a continuous iron enrichment, without any convergence to a single composition. Thus, the range of variability in behavior that may be expected in any given experimental or natural system is at least semi-quantitatively predictable using the simple simulation tools described here.

Implications of the present experimental results for natural systems

The most significant conclusion of this study is that non-volatile major elements as Mg and Fe may be removed (or added) via a ''dry'' vapor phase, which may act as an ''intergranular fluid phase,'' even at moderate temperatures. Thus, it is important to consider the solubility and mobility even of major elements in such vapor or ''intergranular fluid'' phases for petrologic modeling and mass balance calculations. To the extent that major elements are mobilized, it may be necessary to reconsider the metasomatic role of such fluids (e.g., Mg or Fe ''metasomatism'' due to vapor transport in this study). In the particular system addressed in this paper, the extent of solubility of Mg in the vapor phase and ultimately the Fe content of product silicates is determined by the ambient f_{O_2}. This is an example of coupling between various components in such a reaction system. When the role of such an intergranular fluid phase is important, the accessible surface area of the reactants plays a major role in controlling reaction path, progress, and ultimately the products obtained. A special feature of reactions mediated through the gas phase is that the course of the reaction depends on the size of the reacting system or the ''reactive domain.'' It is shown here that in some of these cases, Knudsen-cell mass spectrometry provides a unique opportunity to monitor reaction progress continuously, using several compositional parameters rather than any one single variable. This approach has enabled us to examine the evolution of intergranular fluid phase composition as a function of reaction progress, where the effect was particularly enhanced by physically separating the reactants and thereby magnifying the extent of the ''intergranular fluid'' to an extreme degree. Preliminary high-pressure experiments indicate that the reaction occurs even under pressure and is therefore pertinent to processes within the Earth.

The specific system studied in this work, olivine+iron metal, provides us new insight into several terrestrial and extraterrestrial processes. First, it helps us to explain the enigmatic compositional zoning around FeNi-metal inclusions in olivine from the Allende meteorite. In this context, we emphasize that most of the Ni-Fe inclusions illustrated by Hua et al. (1988) have cracks in their vicinity, which would provide a pathway for the product Mg vapor

to escape. Second, the single-crystal studies of this work provide a mechanism to explain the overgrowth of fayalitic olivine on pre-existing forsterite-rich olivine as seen in Allende and several other meteorites (e.g., Peck and Wood 1987; Hua et al. 1988; Krot et al. 1995). Several mechanisms have been suggested to explain these overgrowths. These include reaction of olivine with aqueous fluid and subsequent dehydration (e.g., Krot et al. 1995; Krot et al. 1997) and reaction of forsterite with a vapor phase containing Fe at an O_2-partial pressure that is higher than that in the canonical solar nebula (e.g., Peck and Wood 1987; Hua and Buseck 1995; Weisberg et al. 1997). It is important to distinguish between these various alternatives, because the choice of the model to explain the fayalitic overgrowths carries implications for the fundamental question: Do mineral assemblages of CV chondrites carry signatures from processes in the solar nebula? In the context of the present study, it is worth noting that all of the previous models were based on thermodynamic equilibrium calculations (e.g., Peck and Wood 1987; Palme and Fegley 1990) and the role of kinetics has been ignored so far. Our experiments and combined thermodynamic-kinetic modeling show that the same process which is required to explain the compositional zoning around metal inclusions in olivine produces fayalite-rich rims on pre-existing olivine under certain conditions. Therefore, if the compositional zoning is to be explained by invoking the escape of Mg in a vapor phase at high temperatures (e.g., in the solar nebula), it is difficult to avoid producing at least some fayalite-rich rims on pre-existing olivine from the same vapor phase. This process has been studied in further detail and the results will be discussed elsewhere (Dohmen et al. in preparation). Third, similar reactions may play an important role in the textural development through diffusion-controlled processes in other meteorites bearing olivine+metal such as the pallasites studied by Ohtani (1983) and Saiki et al. (1996). Fourth, we need to consider the possible effects of such Mg or Fe ''metasomatism'' during core formation in the Earth, in the terrestrial magma ocean during the early history of the Earth, and at the core-mantle boundary region (D'' layer) within the present-day Earth.

The reaction modeling shows that the observed behavior of the system olivine plus iron metal does not result from any system-specific surface properties, but follows simply from thermodynamic data. Thus, similar behavior for other minerals at various *P-T* conditions are predictable using thermodynamic data, and the observations of this study are therefore generally applicable to reactions between solids in the presence of a vapor phase.

Acknowledgments

We thank C. Petry for help in the lab and reviewers R. Colson, J. Ganguly, A. Krot, and associate editor B. Jolliff for their constructive criticism. Some of the element mapping was done at the Bayerisches Geoinstitut, Bayreuth and the BSE images were collected using a SEM at Institut für Planetologie, Münster. We thank these institutions for the access to the equipment.

References cited

Abbott, N.M. and Van Ness, H.C. (1972) Thermodynamics: Schaum's outline series in engineering, 346 p. McGraw-Hill, New York.

Carmichael, D.M. (1969) On the mechanisms of prograde metamorphic reactions in quartz-bearing pelitic rocks. Contributions to Mineralogy and Petrology, 20, 244–267.

Chakraborty, S. (1997) Rates and mechanisms of Fe-Mg interdiffusion in olivine at 980–1300 °C. Journal of Geophysical Research, 102, 12317–12331.

Chakraborty, S., Farver, J.R., Yund, R.A., and Rubie, D.C. (1994) Mg tracer diffusion in synthetic forsterite and San Carlos Olivine as a function of P, T, and f_{O_2}. Physics and Chemistry of Minerals, 21(8), 489–500.

Erambert, M. and Austrheim, H. (1993) The effect of fluid and deformation on zoning and inclusion patterns in poly-metamorphic garnets. Contributions to Mineralogy and Petrology, 115, 204–214.

Fisher, G.W. (1973) Nonequilibrium thermodynamics as a model for diffusion-controlled metamorphic processes. American Journal of Science, 273, 897–924.

Foster, C.T. Jr. (1977) Mass transfer in sillimanite-bearing pelitic schists near Rangeley, Maine. American Mineralogist, 62, 727–746.

Fraser, D.G. and Rammensee, W. (1982) Activity measurements by Knudsen cell mass spectrometry—the system Fe-Co-Ni and implications for condensation processes in the solar nebula. Geochimica et Cosmochimica Acta, 46, 549–556.

Hashimoto, A. (1990) Evaporation kinetics of forsterite and implications for the early solar nebula. Nature, 347, 53–55.

Hua, X. and Buseck, P.R. (1995) Fayalite in the Kaba and Mokoia carbonaceous chondrites. Geochimica et Cosmochimica Acta, 59, 563–578.

Hua, X., Adam, J., Palme, H., and El Goresy, A. (1988) Fayalite-rich rims, veins, and halos around and in forsteritic olivines in CAI's and chondrules in carbonaceous chondrites: Types, compositional profiles and constraints of their formation. Geochimica et Cosmochimica Acta, 52, 1389–1408.

JANAF (1971) Thermochemical tables, Second Edition. Stull, D.R. and Prophet, H., U.S. Government Printing Office, Washington, D.C.

Krot, A.N., Scott, E.R., and Zolensky, M.E. (1995) Mineralogical and chemical modification of components in CV3 chondrites: Nebular or asteroidal processing? Meteoritics, 30, 748–775.

———(1997) Origin of fayalitic olivine rims and lath-shaped matrix olivine in the CV3 chondrite Allende and its dark inclusions. Meteoritics and Planetary Science, 32, 31–49.

Loomis, T.P. (1976) Irreversible reactions in high-grade metapelitic rocks. Journal of Petrology, 17, 559–588.

———(1977) Kinetics of a garnet granulite reaction. Journal of Petrology, 62, 1–22.

———(1979) A natural example of metastable reactions involving garnet and sillimanite. Journal of Petrology, 20, 271–292.

Mysen, B.O. and Kuhiro, I. (1988) Condensation, evaporation, melting, and crystallization in the primitive solar nebula: Experimental data in the system MgO-SiO_2-H_2 to 1.0×10^{-9} bar and 1870 °C with variable oxygen fugacity. American Mineralogist, 73, 1–19.

Nagahara, H., Kushiro, I., and Mysen, B.O. (1994) Evaporation of olivine: Low pressure phase relations of the olivine system and its application for the origin of chondritic components in the solar nebula. Geochimica et Cosmochimica Acta, 58, 1951–1963.

Nichols, R.H.J., Wasserburg, G.J., and Grimley, R.T. (1995) Evaporation of forsterite: Identification of gas-phase species via Knudsen cell mass spectrometry. Lunar and Planetary Science Conference XXVI, 1047–1048.

Ohtani, E. (1983) Formation of olivine textures in pallasites and thermal history of pallasites in their parent body. Physics of Earth and Planetary Interiors, 32, 182–192.

Orville, P.M. (1962) Alkali metasomatism and feldspars: Norsk geologisk tidsskrift, 42, 283–316.

———(1963) Alkali ion exchange between vapor and feldspar phases. American Journal of Science, 261, 201–237.

O'Brien, P.J. (1997) Granulite facies overprint of eclogites: Short-lived

events deduced from diffusion modeling. Proceedings of the 30th International Geological Congress, Beijing, China.
Palme, H. and Fegley, B. Jr. (1990) High-temperature condensation of iron-rich olivine in the solar nebula. Earth and Planetary Science Letters, 101, 180–195.
Peck, J. and Wood, J.A. (1987) The origin of ferrous zoning in Allende chondrule olivines. Geochimica et Cosmochimica Acta, 51, 1503–1510.
Rammensee, W. (1988) Die Knudsenzellenmassenspektrometrie: Prinzipien, Entwicklungen und Anwendungen in der geowissenschaftlichen Forschung, 152 p. Habilitationsschrift, Universität Göttingen, Germany.
Rammensee, W. and Fraser, D.G. (1981) Activities in solid and liquid Fe-Ni and Fe-Co alloys determined by Knudsen cell mass spectrometry. Berichte der Bunsengesellschaft Physikalische Chemie, 85, 588–592.
Robie, R.A., Hemingway, B.S., and Fisher, J.R. (1979) Thermodynamic properties of minerals and related substances at 298.15 K and 1 bar pressure and at higher temperatures, 456 p. U.S. Geological Survey Bulletin 1452, Washington D.C.
Saiki, K., Laporte, D., Boivin, P., Vielzeuf, D., and Nakashima, S. (1996) An experimental study of the rounding process of olivine in Fe-Ni metal. Terra Nova Abstracts, 8, 57.
Schmalzried, H. (1995) Chemicals kinetics of solids, 433p. VCH Verlag, Weinheim, Germany.
Smith, D. (1996) Thin film deposition, 616 p. McGraw-Hill, New York.
Smith, W.R. and Missen, R.W. (1991) Chemical reaction equilibrium analysis: Theory and algorithms, 364 p. Krieger Publishing Company, Malabar, Florida.
Srecec, I., Ender, A., Woermann, E., Gans, W., Jacobsson, E., Eriksson, G., and Rosen, E. (1987) Activity-composition relations of the magnesiowüstite solid solution series in equilibrium with metallic Iron in the temperature range 1050–1400 K. Physics and Chemistry of Minerals, 14, 492–498.
Weinbruch, S., Palme, H., Müller, W.F., and El Goresy, A. (1990) FeO-rich rims and veins in Allende forsterite: Evidence for high temperature condensation at oxidizing conditions. Meteoritics, 25, 115–125.
Weisberg, M.K., Zolensky, M.E., and Prinz, M. (1997) Fayalitic olivine in matrix of the Krymka LL3.1 chondrite: Vapor-solid growth in the solar nebula. Meteoritics and Planetary Science, 32, 791–801.
Wiser, N.M. and Wood, B.J. (1991) Experimental determination of activities in Fe-Mg olivine at 1400 K. Contributions to Mineralogy and Petrology, 108, 146–153.
Zipfel, J. and Wörner, G. (1992) Four- and five-phase peridotites from a continental rift system: evidence for upper mantle uplift and cooling at the Ross Sea margin (Antarctica). Contributions to Mineralogy and Petrology, 111, 24–36.
Zipfel, J., Palme, H., Kennedy, A.K., and Hutcheon, I.D. (1995) Chemical composition and origin of the Acapulco meteorite. Geochimica et Cosmochimica Acta, 59, 3607–3627.

Manuscript received July 7, 1997
Manuscript accepted April 15, 1998
Paper handled by Brad L. Jolliff